ELSEVIER

Journal of Nuclear Materials 278 (2000) 186–194

journal of nuclear materials

www.elsevier.nl/locate/jnucmat

Effect of composition on the fatigue failure behavior of vanadium alloys

H.A. Aglan [a,*], Y.X. Gan [a], B.A. Chin [b], M.L. Grossbeck [c]

[a] *Mechanical Engineering Department, Tuskegee University, Tuskegee, AL 36088, USA*
[b] *Center for Materials Research and Education, Auburn University, Auburn, AL 36849, USA*
[c] *Oak Ridge National Laboratory, Oak Ridge, TN, USA*

Received 22 June 1999; accepted 8 October 1999

Abstract

In this work, the effect of composition on the fracture surface morphology and fatigue failure behavior of two vanadium alloys (V–4Ti–4Cr and V–5Ti–5Cr) under cyclic tensile loading was investigated. In the beginning of the stable crack growth stage, the crack speed for both vanadium alloys is very close; however, in the remainder of the stable crack growth stage, and the unstable crack stage, the crack speed for V–5Ti–5Cr is higher than that for V–4Ti–4Cr. The fracture surface features in the stable crack propagation region of the V–4Ti–4Cr show fatigue striations, drawn-out material, micro-cracks and micro-voids, indicating the various damage species associated with stable fatigue crack growth. The V–5Ti–5Cr, on the other hand, displayed twinning, cleavage tongues and tearing steps, in addition to slip in the stable crack propagation region of its fracture surface. Plastic deformation and ductile fracture mechanisms characterized by tearing and void coalescence can also be observed on the fracture surface in the fast crack region of the V–4Ti–4Cr. Nevertheless, the V–5Ti–5Cr shows more inter-granular fracture and quasi-cleavage features in the fast crack propagation region. It was also found that the specific energy of damage (γ'), a material parameter characteristic of the alloys' fatigue fracture resistance, is composition dependent. A 1% increase of both the Ti and Cr content resulted in about a 30% reduction in the value of γ'. This has also resulted in a significant change in the fracture surface morphology and the fatigue fracture mechanisms.

1. Introduction

Metallic materials deform in several ways under cyclic loads among which slip and twinning are very common [1]. Slip is a coherent movement of atoms in a layer relative to another layer and can occur within grains or along the grain boundaries [2,3]. Persistent slip results in slip strips or deformation bands as observed in many ductile metallic alloys [4,5]. Localized plastic deformation or appreciable surface displacement was also observed due to continuous slip [6,7]. Materials with small angle grain boundaries normally display lower strength but higher ductility and toughness than those with large angle grain boundaries, due to the frequent slip movement along the small angle grain boundaries under loading [8].

Twinning is a complex atomistic rearrangement process of crystals under loading. Twinning often occurs in body-centered cubic (bcc) crystalline metals or alloys. Hexagonal close-packed (hcp) metallic materials can also respond to external loading by twinning. However, twinning rarely occurs in face-centered cubic (fcc) metals and alloys, since there are many slip bands in fcc crystals. During the twinning process, the movement of the lattice along a preferential plane produces the same kind of crystalline structure, and is symmetrical to the other part as a mirror image across the plane. The preferential plane is called the twinning plane, and the crystal on one side of the plane is a twin of that on the other side [1]. Twinning can form sub-grain boundary [9], and lamella texture [10]. Twinning can also play a role in fatigue crack initiation [1].

* Corresponding author. Tel.: +1-334 727 8973; fax: 1-334 727 8090.
E-mail address: aglanh@acd.tusk.edu (H.A. Aglan).

0022-3115/00/$ - see front matter
PII: S0022-3115(99)00258-5

Different failure mechanisms corresponding to slip and twinning can be found in metallic alloys. Slip can produce the separation of materials internally besides surface displacement. The internal discontinuities form voids then join or coalesce to form the fracture surface. Ductile fracture features can be observed in such a case as for many metals and alloys [11,12]. Generally, the voids form at either soft or hard second-phase particles by de-cohesion of the particle/matrix interface or by fracture of the particles [13]. In multi-crystalline materials, voids nucleate along grain boundaries and then cracking occurs. This is the typical dimpled grain boundary fracture [14].

Cleavage, on the other hand, is related to twinning deformation [15]. Specifically, in bcc metals and/or alloys, the formation of twins leads the crack front to deviate by separation of the plane between the twin and the matrix material. Thus, trans-granular cleavage facets remain on the fracture surface. Quasi-cleavage fracture as a mixed mechanism has also been found in many metallic materials [16,17], particularly in bcc structures. The major characteristic is the cleavage accompanied by ductile tearing or dimples. This type of failure mode develops by the formation of micro-cracks and then extensive plastic deformation of the remaining material.

Inter-granular fracture occurs when the grain boundaries in materials become weak zones [18]. In some complex micro-structures containing particles and second phase interfaces, inter-granular fracture was often observed [19]. Inter-granular fracture can be along particles or dimples distributed in a weak zone adjacent or parallel to the boundaries. Since grain boundaries are especially sensitive to environmental factors such as corrosive substances, hydrogen embrittlement, inter-granular fracture or separation often occurs under such conditions. Impurity segregation can also promote inter-granular fracture. Investigation into the fracture behavior of some materials shows the transition of fracture mechanisms from one form to another, for example, from trans-granular to inter-granular or from inter-granular to trans-granular [20–22]. This is particularly manifested when the amount of an element in the material system is changed [23].

Vanadium alloys, a new class of metallic materials, have been considered for use in the field of nuclear power generation. However the effect of composition on the fracture and fatigue behavior have not been fully studied. It was found that the mechanical behavior of vanadium alloys depends on the amount of alloying elements [24,25]. Recent studies have shown that the ternary alloy system of vanadium–titanium–chromium has significant importance in the development of vanadium alloys. Addition of a small amount of titanium can improve the ductility of the vanadium alloys. Titanium can act as a deoxidizer; removing soluble oxygen and nitrogen in the form of dispersed sub-oxides and nitrides [26,27]. The addition of chromium can increase the strength [24] without affecting the forgeability of the alloys.

Vanadium alloys, with titanium and chromium as basic alloying elements, have found promising applications especially as candidate materials for tritium breeding blankets and in the first wall of fusion reactors [28,29]. V–Ti–Cr alloys possess weldability by means of argon-arc welding with enhanced protection, as well as electron-beam welding. Welded joints of vanadium alloys are rather resistant to the formation of hot cracks and the weldment of vanadium alloys do not need any additional heat treatment [24]. In addition to the above advantages, the chemical inertness of V–Ti–Cr alloys in liquid metals, such as lithium and lithium based alloys, is very important for structural applications in fusion reactors. The mechanical properties of such alloys are stable under the simulated lithium circulating conditions. Vanadium alloys with titanium and chromium can trap or lead to localization of nitrogen impurities absorbed from lithium in fine surface layers where it is present in the form of titanium nitride (TiN) [28]. The TiN film, with dense structure and extremely high inertness, is protective and prevents an increase in the rate of the metal mass transfer. Experimental studies performed by Evtikhin and Lyublinski [30] revealed that the mass transfer of the V–Ti–Cr system alloy by means of lithium flow containing the nitrogen impurity up to 500 ppm is substantially lower than permissible values. V–Ti–Cr alloy has very low activity when exposed to high temperature water-steam circulation in heat exchangers. This is due to the formation of the fine passive oxide films such as TiO_2 and Cr_2O_3. These passive films are highly protective by impeding the process of hydrogen saturation of alloys [31].

Characterization of the mechanical properties of vanadium alloys reveals ductile behavior under monotonic over-loadings at various testing temperatures [32]. The V–Ti–Cr system shows an ideal combination of low room temperature strength and high ductility, high elevated temperature strength and non-heat-treatability [28]. Studies of the tensile properties at ambient and elevated temperatures have demonstrated that the percentage of titanium in binary alloys for optimum strength decreases with the increase of temperature. The tensile strength of V–Ti alloys at elevated temperatures can be enhanced by a third metal such as chromium. Stress rupture data have been acquired for V–Ti–Cr alloys for further evaluation of the high temperature fracture behavior and creep. At temperature ranges from 500°C to 700°C, it was found that the stress rupture limits are highly temperature dependent, and higher contents of titanium with third metal addition are very useful for increasing the creep strength [24].

The tensile properties of vanadium alloys can be affected by radiation. Increase in ultimate tensile strength

and yield strength of several alloy systems including V–Ti–Cr alloys have been observed after neutron irradiation at temperatures of 400–700°C to considerably high fluences in the range 10^{21}–10^{23} cm^{-1}. The plasticity of all the vanadium alloys decreases after irradiation. V–15Ti–7.5Cr alloy, demonstrated up to a 25% increase in yield strength at 600°C, after having been irradiated at the same temperature [32]. The tensile properties of V–Ti–Cr ternary alloys are relatively stable over a temperature range from 25°C to 800°C. The increase in strength is observed after irradiation [33]. Nevertheless, the high temperature creep rate can be increased upon irradiation [28]. It was also found that irradiation can cause both low temperature embrittlement and high temperature embrittlement, thus degrading the mechanical properties of vanadium alloys. The low temperature embrittlement occurs at temperatures lower than 300°C; while the high temperature embrittlement appears in the temperature range 700–1000°C. Titanium is effective in suppressing the low temperature embrittlement, and chromium has the function of alleviating the high temperature embrittlement. Furthermore, the titanium can also reduce the swelling tendency of vanadium alloys during irradiation [34].

The effect of composition on the fatigue behavior of vanadium alloys has had very little focused research, and data on the fatigue properties are extremely limited. Comparative studies on the fatigue behavior of stainless steel and vanadium alloys have been performed [35]. Vanadium alloys of V–Ti–Cr and V–Cr–Fe–Zr systems were fatigue tested under various temperature conditions including room temperature, 550°C and 650°C. The fatigue properties of the V–Cr–Fe–Zr alloy system are inferior to that of the V–Ti–Cr alloys, namely V–5Ti–15Cr at the three test temperatures. The fatigue lifetime of unalloyed vanadium at room temperature has been found to change with the hydrogen content [36]. The crack initiation lifetime increases with the increase of hydrogen content; while the propagation lifetime decreases. These limited data appear to be insufficient for understanding the effect of each alloying and extraneous element on the fatigue crack resistance. In addition, the related fracture and fatigue failure mechanisms of V–Ti–Cr alloys especially the V–4Ti–4Cr and V–5Ti–5Cr have not been studied. In the present work, the effect of composition on the fracture and fatigue failure behavior of V–4Ti–4Cr and V–5Ti–5Cr alloys has been investigated. Tension–tension fatigue experiments followed by microscopic examination of the fatigue fracture surface of each alloy was performed to identify the fracture mechanisms and the associated damage species. The specific energy of damage (γ') [37], a material constant characteristic of the fatigue fracture resistance was generated for each material and its dependency on composition was established.

2. Materials and experimental

The materials used in the present work are V–4Ti–4Cr and V–5Ti–5Cr alloys, manufactured by Wah Chang of Albany, OR, with heat numbers 832864 and 832394 respectively. Rectangular specimens 60 mm × 12.5 mm × 1 mm were machined. An initial 1.25 mm 60° V-notch was introduced at the center of one free edge. Fatigue pre-cracking was performed until the crack length reached 3.0 mm. The fatigue tests were conducted at room temperature under load control conditions at a frequency of 3 Hz using an MTS 810 hydraulic testing machine. A sinusoidal wave form was used with a maximum tension stress of 130 MPa, and a minimum tension stress of 13 MPa. The crack length at various intervals of number of cycles was measured optically using a video camera with a zoom lens connected to a video system. For each material, a total of three samples were tested. The fatigue fracture surfaces of each material were examined using a Hitachi S-2150 scanning electron microscope.

3. Results and discussion

3.1. Composition–fatigue fracture morphology relationship

The fatigue fracture surface for typical V–4Ti–4Cr and V–5Ti–5Cr samples is shown schematically in Fig. 1. The notch is at the left-hand side of the samples. The crack propagation direction is from left to right. In addition to the threshold region produced in the pre-cracking stage, the fracture surface can be divided into two regions according to the morphological features observed. The stable crack region is about 7 mm in length. In the beginning of this region, both V–4Ti–4Cr and V–5Ti–5Cr display some roughness on the fracture surface. A micrograph, Fig. 2, taken from location 'A' in Fig. 1, for V–4Ti–4Cr shows cavitation and micro-void coalescence. Such a feature is generally formed under slip and ductile tearing [38]. Fine ridgelines along the crack growth direction are clearly shown in Fig. 2,

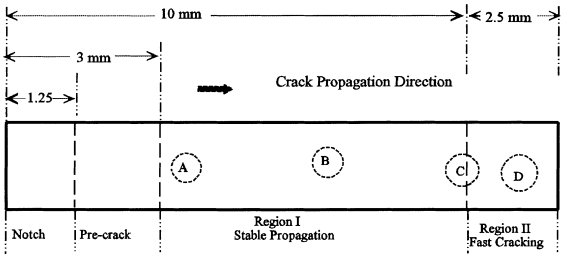

Fig. 1. Schematic representation of the fatigue fracture surface showing the various regions and locations of the microscopic examination.

indicating a high energy consuming process associated with the crack growth in the beginning of the stable crack region in the V–4Ti–4Cr alloy. In the V–5Ti–5Cr alloy a mixed mechanism of ductile tearing and cleavage was found as shown in Fig. 3; a micrograph taken from the same location 'A' as shown in Fig. 1. Although some cleavage tongues, similar to other metallic alloys [39], are clearly shown in Fig. 3, the ductile tearing is the major failure mechanism which is very common in most metallic materials containing alloy elements [40].

In the middle of the stable crack propagation region, location B in Fig. 1, the fracture surfaces of each of the two vanadium alloys display extensive plastic deformation associated with the crack growth. This indicates that slip deformation mechanism exists during the fatigue fracture process. This feature is more evident in the V–4Ti–4Cr as shown in Fig. 4; a micrograph taken from location 'B' in Fig. 1. Drawn-out ridges in the form of elongated 'strips', microcracks, inter-crystalline separation and ill-defined fatigue striations are the major fracture surface features of the V–4Ti–4Cr alloy. An SEM micrograph for the V–5Ti–5Cr, Fig. 5, shows a considerably rough fracture surface with no obvious fatigue striations. Pulled-up material due to slip and tearing, twinning, and cleavage tongues can also be found. In addition, several cleavage facets due to the inter-granular fracture are seen on the fracture surface of the V–5Ti–5Cr alloy in the middle of the stable crack growth region.

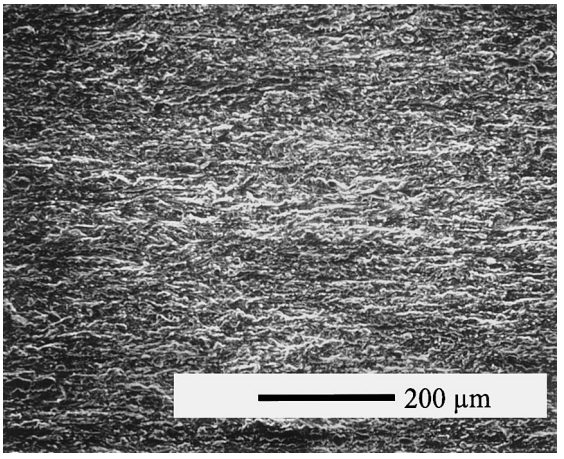

Fig. 2. An SEM micrograph taken from the beginning of the stable crack propagation region of the V–4Ti–4Cr, showing fine ridge lines.

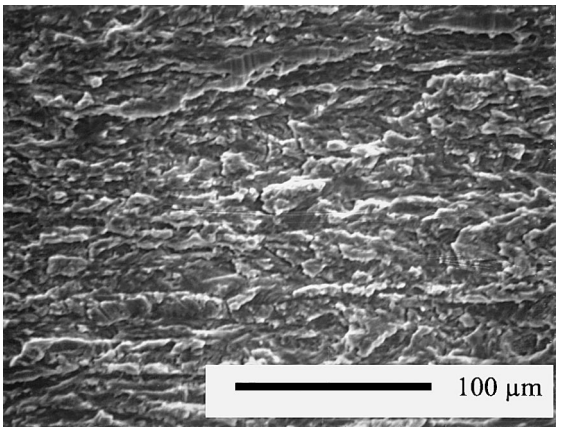

Fig. 4. An SEM micrograph taken from the middle of the stable crack propagation region for the V–4Ti–4Cr, showing tearing ridges, microcracks, and elongated strips.

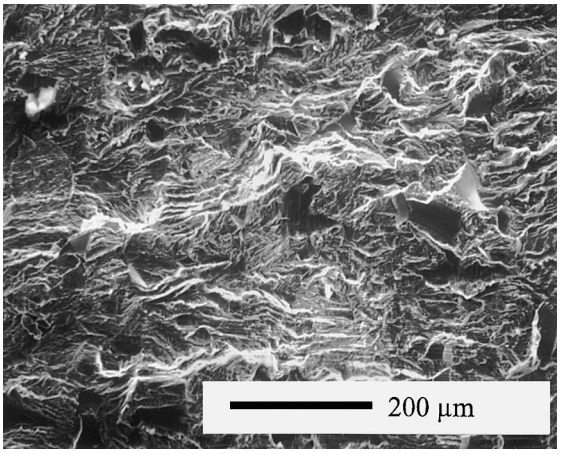

Fig. 3. An SEM micrograph taken at the beginning of the stable crack propagation region of the V–5Ti–5Cr, showing mixed fracture mechanism characterized by ductile tearing and cleavage tongues.

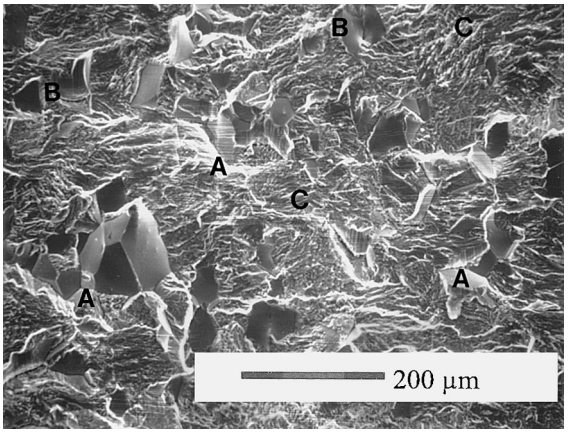

Fig. 5. An SEM micrograph taken from the middle of the stable crack propagation region for the V–5Ti–5Cr, showing twinning (at A), cleavage tongues (at B) and pull-up materials due to slip and tearing (at C).

Location C, as shown in Fig. 1, represents the transition zone between the stable and unstable crack growth regions. Fig. 6, an SEM micrograph for the V–4Ti–4Cr alloy taken from this location shows the fracture surface of the transition zone. The left side of the micrograph, the end of the stable crack region, contains tearing ridges and microvoids. The right side of Fig. 6, the beginning of the unstable crack growth region, is comprised of dimples (top) and a shear lip (bottom). For the V–5Ti–5Cr alloy, the fracture surface in its transition zone reveals more cleavage features. Inter-granular separation, mechanical twinning, and cleavage facets are clear in the right side of the micrograph in Fig. 7. Tearing ridges, ill-defined fatigue striations and secondary microcracks are the major features in the left side of Fig. 7. Much fewer slip and tearing features can be observed in Fig. 7, which suggests that the fracture mechanism in this region is more brittle-like. It is also obvious that with the increase in the content of both Ti and Cr, vanadium alloys demonstrate the transition in the fracture mechanism from a ductile mode to mixed mode, which is also observed in some low carbon content steels [41].

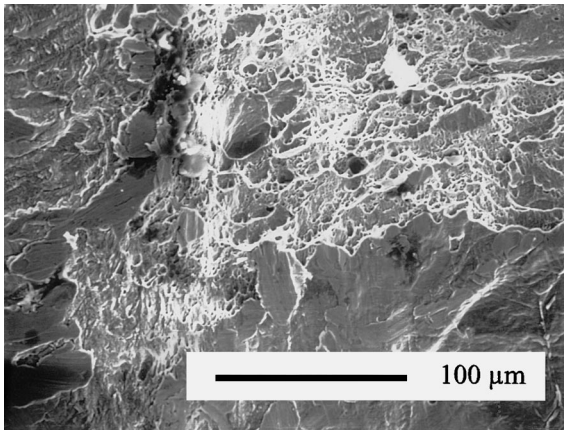

Fig. 6. An SEM micrograph taken from the transition zone of the V–4Ti–4Cr, showing tearing ridges and intergranular voids as well as dimples.

The unstable crack growth region of both vanadium alloys, location D in Fig. 1, was also examined. The V–4Ti–4Cr shows a slanted fracture surface with a single shear lip, as described previously [42–44]. However, no shear lips were found in the unstable crack propagation region of the V–5Ti–5Cr. Typical fracture surface morphologies, associated with the unstable crack region for both V–4Ti–4Cr and V–5Ti–5Cr alloys, are shown in Figs. 8 and 9, respectively. These micrographs were taken from location 'D' in Fig. 1. From Fig. 8, the micrograph for V–4Ti–4Cr, it can be seen that plastic deformation was produced in the final stage of the fatigue crack propagation. The material was extensively drawn-out and numerous equiaxed tensile dimples with diversified sizes are shown in Fig. 8. All these fracture surface features demonstrate a ductile fracture mechanism in the V–4Ti–4Cr. The fracture surface morphology of the V–5Ti–5Cr in the unstable crack growth region displays completely different features in comparison with that of the V–4Ti–4Cr alloy. Fig. 9, an SEM micrograph for the V–5Ti–5Cr taken from the same location 'D', clearly shows cleavage facets, river patterns, and inter-granular secondary cracks. The more obvious inter-granular fracture surface may be due to the precipitation in the grain boundaries. Normally, aggregated precipitates along grain boundaries will promote the inter-granular fracture [45–47]. This can be the explanation of the more

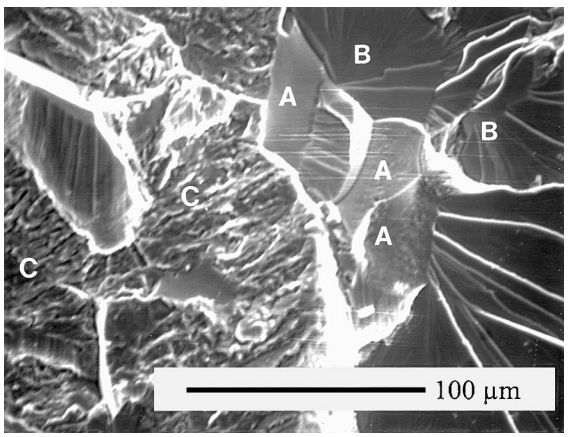

Fig. 7. An SEM micrograph taken from the transition zone of the V–5Ti–5Cr, showing cleavage facets (at A), twinning (at B) and tearing (at C).

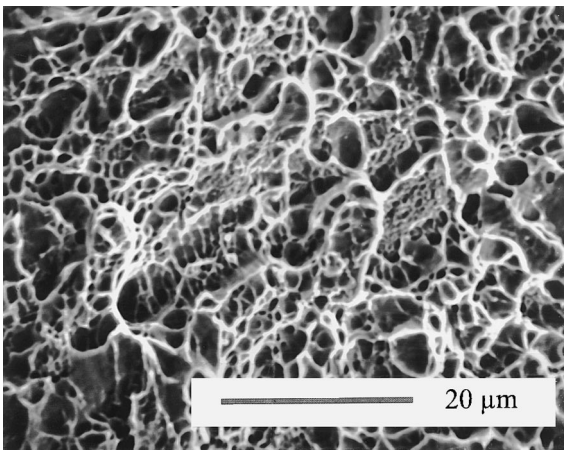

Fig. 8. An SEM micrograph taken from the unstable cracking region of the V–4Ti–4Cr showing numerous equiaxed dimples.

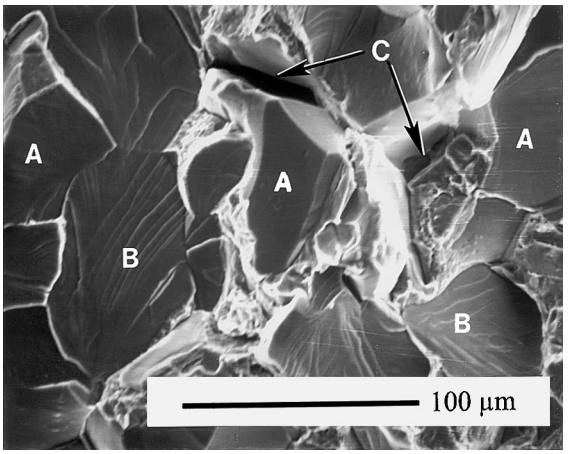

Fig. 9. An SEM micrograph taken from the unstable cracking region of the V–5Ti–5Cr featured by cleavage facets (at A), river patterns (at B), and inter-granular separation (at C).

brittle fracture behavior of the V–5Ti–5Cr in the final stage of the fatigue crack propagation.

3.2. Composition–fatigue crack propagation kinetics relationship

The relationship between the crack length, a, and the number of cycles, N, for both V–4Ti–4Cr and V–5Ti–5Cr is shown in Fig. 10. It can be seen that the total fatigue lifetime of the V–4Ti–4Cr alloy is approximately 130,000 cycles, while that for the V–5Ti–5Cr, is only about 95,000 cycles. In the fatigue crack length range of 3 to 5.5 mm, the two vanadium alloys almost have the same fatigue behavior. It takes about 80 000 cycles for the two materials to reach the same crack length of 5.5 mm. Beyond 5.5 mm crack length, the a–N curve of the V–5Ti–5Cr is steeper than that of the V–4Ti–4Cr. This indicates that the crack propagated faster in the V–5Ti–5Cr than in the V–4Ti–4Cr.

The relationship between the crack speed, da/dN, and crack length, a, for both vanadium alloys is shown in Fig. 11. This relationship was used instead of da/dN versus ΔK (the stress intensity factor range) in order to correlate the FCP kinetics with the fracture surface features at different crack lengths. The curves in this figure display two stages of crack growth kinetics. The first stage corresponds to the stable crack propagation, while the second stage demonstrates the unstable crack growth. In the first stage, a considerably slow crack growth behavior is observed. It is due to the damage formation and evolution in the vicinity of the main crack. This has been confirmed by the fracture surface features identified in Figs. 2 and 3. The two curves approached asymptotic values in the unstable crack growth stage. It must be noted that before the first region, there exists threshold behavior in the cyclic process of the pre-crack formation, as commonly observed in the fatigue of other metallic materials [48,49]. This was also shown in our earlier work on the V–4Ti–4Cr [42]. A comparison of the crack speed of the two vanadium alloys indicates that in the beginning of the stable crack propagation stage, the crack growth rate for both V–4Ti–4Cr and V–5Ti–5Cr is very close. At the crack

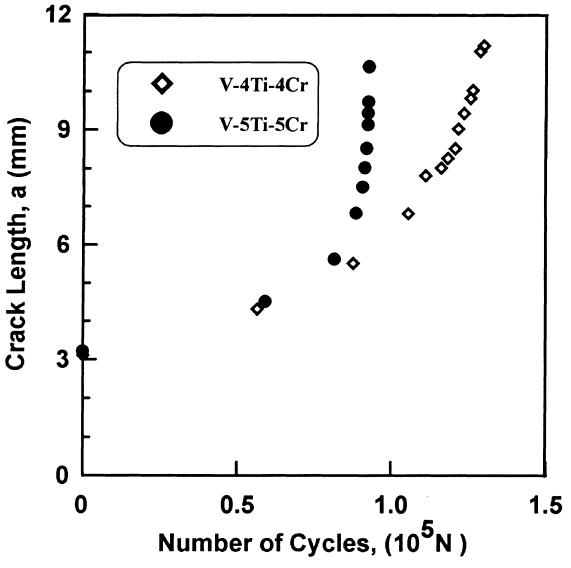

Fig. 10. Fatigue crack length, a, versus the number of cycles, N, for the V–4Ti–4Cr and V–5Ti–5Cr alloys.

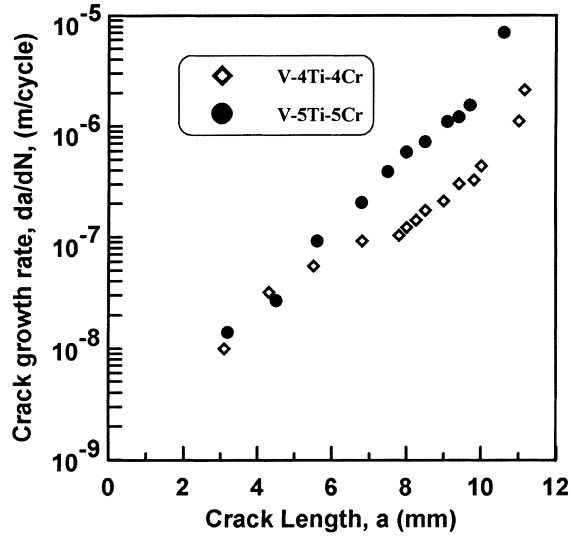

Fig. 11. Fatigue crack propagation speed, da/dN, versus crack length, a, for the V–4Ti–4Cr and V–5Ti–5Cr alloys.

length of 3 mm, both alloys have a crack speed of about 1.0×10^{-8} m/cycle. As the crack moves, the crack speed increases for both alloys. When the crack length increases from 3 to 4.5 mm, the crack speed increases to 3.0×10^{-8} m/cycle for both alloys. Above a crack length of 5 mm there exists a difference between the crack growth rate for the two vanadium alloys. The V–5Ti–5Cr alloy shows higher crack speed than the V–4Ti–4Cr at any crack length above 5 mm. This is attributed to the mixed fracture mechanisms of ductile tearing and cleavage associated with the V–5Ti–5Cr alloys.

3.3. Composition-fatigue crack growth resistance relationship

The specific energy of damage, γ', a material parameter characteristic of the V–4Ti–4Cr and V–5Ti–5Cr alloys' resistance to fatigue crack growth, was generated using the Modified Crack Layer (MCL) theory [42]. In this analysis, the crack length, a, crack speed, da/dN, the energy release rate J^*, and the change in work $\dot{W}_i$, were employed for the evaluation of γ'. The procedures for the evaluation of γ', have previously been demonstrated [37,42,50,51]. According to the MCL theory, plots of J^*/a versus $\dot{W}_i/[a(\mathrm{d}a/\mathrm{d}N)]$ for the two vanadium materials should give two separate straight lines, with γ' being the intercept of the lines. This is shown in Fig. 12. The values of γ' for the V–4Ti–4Cr and V–5Ti–5Cr were found to be 2500 and 1700 kJ/m^3, respectively. A higher value of γ' indicates higher resistance of the material to crack growth, since more energy is required to cause a unit volume of the material to change from an undamaged state to a damaged state. This suggests that the V–4Ti–4Cr has a higher fatigue fracture resistance than the V–5Ti–5Cr.

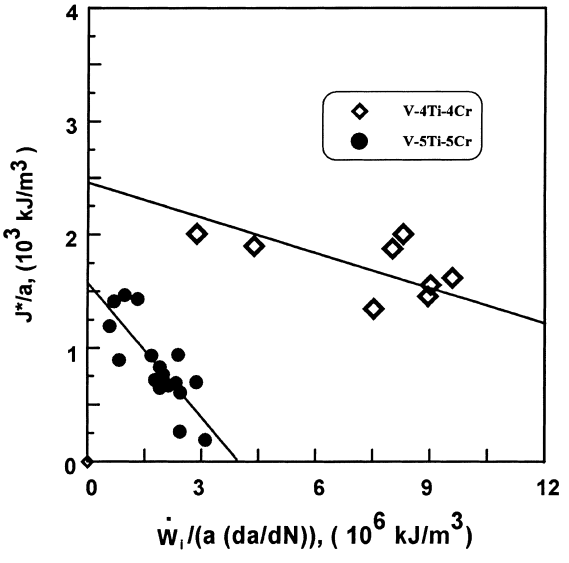

Fig. 12. Fatigue crack propagation data to obtain γ' using the Modified Crack Layer (MCL) theory.

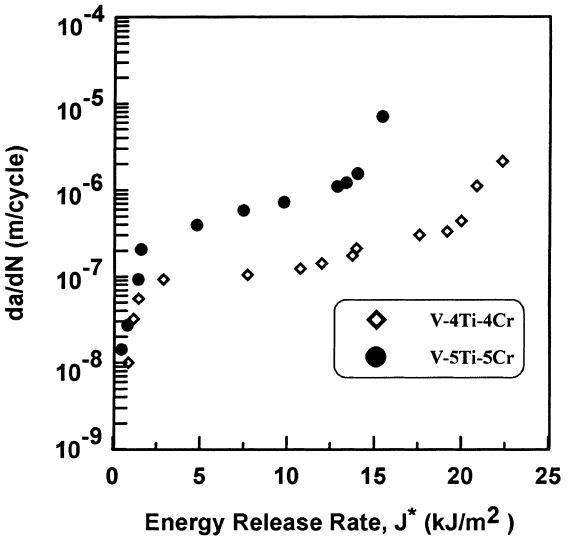

Fig. 13. The fatigue crack propagation speed versus the energy release rate for the V–4Ti–4Cr and V–5Ti–5Cr alloys.

The crack speed versus the energy release rate for the V–4Ti–4Cr and V–5Ti–5Cr alloys is shown in Fig. 13. It can be seen from this figure that as the energy release rate increases, the crack speed, da/dN, increases. The two curves display similar fatigue crack propagation behavior, a stable crack propagation stage followed by a stage of unstable crack propagation over almost the entire energy release rate range. The tendency of the fatigue crack propagation kinetics is basically in agreement with the calculated results of crack speed, da/dN, versus crack length, a, as shown in Fig. 11. The dependency of the FCP kinetics on the composition is also shown in Fig. 13. It is clear that the V–5Ti–5Cr demonstrates faster crack speed than the V–4Ti–4Cr over almost the entire energy release rate range. Thus, the higher the content of Ti and/or Cr, the higher the crack speed. This is in agreement with the results of the fracture surface morphology examination and fracture mechanisms analysis of these two alloys.

4. Conclusions

It was found that the fatigue fracture surface morphologies of the vanadium alloys are composition dependent. In the beginning of the stable crack region, the fracture surface of V–4Ti–4Cr shows a great number of micro-cracks, voids, and drawn-out material indicating fatigue damage evolution and high energy consumption during FCP, while the V–5Ti–5Cr demonstrates twin-

ning, cleavage tongues and tearing steps. In the stable–unstable crack transition area, the V–4Ti–4Cr demonstrated a ductile fracture mechanism, while the V–5Ti–5Cr shows quasi-cleavage features. The unstable crack of V–4Ti–4Cr is characterized by ductile fracture features with dimple formation associated with extensive plastic deformation. The V–5Ti–5Cr, on the other hand, displayed brittle fracture features in the form of cleavage and inter-granular separation.

The fatigue failure behavior and fracture mechanisms of vanadium alloys showed strong composition dependency. Two distinct fatigue fracture stages can be observed, a stable crack stage followed by an unstable crack propagation stage. The higher the alloy composition, the faster the fatigue crack growth. The specific energy of damage, γ', a material parameter characteristic of the vanadium alloys' resistance to FCP was found to be dependent on the alloy composition. A 1% increase of both the Ti and Cr content resulted in about a 30% reduction in the value of γ'. The drop in resistance is manifested by the quasi-brittle morphological features observed on the fracture surface of the V–5Ti–5Cr alloy.

Acknowledgements

This work was supported by US Department of Energy (DOE) under contract number E-FG02-96ER54384.

References

[1] C.R. Brooks, A. Choudhury, Metallurgical Failure Analysis, McGraw-Hill, New York, 1993, p. 120.
[2] O.A. Kaibyshev, A.I. Pshenichniuk, V.V. Astanin, Acta Mater. 46 (1998) 4911.
[3] Y. Koizumi, T. Nakano, Y. Umakoshi, Acta Mater. 46 (1998) 4743.
[4] X.W. Li, Z.G. Wang, G.Y. Li, S.D. Wu, S.X. Li, Acta Mater. 46 (1998) 4497.
[5] P. Hahner, B. Tippelt, C. Holste, Acta Mater. 46 (1998) 5073.
[6] B. Liao, Y. Nan, Y. Hu, D.T. Kang, J. Mater. Eng. Performance 7 (1998) 100.
[7] W.W. Gerberich, S.E. Harvey, D.E. Kramer, J.W. Hoehn, Acta Mater. 46 (1998) 5007.
[8] Z.F. Zhang, Z.G. Wang, Acta Mater. 46 (1998) 5063.
[9] J. Shen, R. Balasubramanian, D.K. Aidun, L.L. Regel, W.R. Wilcox, J. Mater. Eng. Performance 7 (1998) 555.
[10] D.H. Hanlon, W.M. Rainforth, C.M. Sellars, R. Price, H.T. Gisborne, J. Forrest, J. Mater. Sci. 33 (1998) 3233.
[11] D.M. Lipkin, D.R. Clarke, A.G. Evans, Acta Mater. 46 (1998) 4835.
[12] J. Dille, J. Charlier, R. Winand, J. Mater. Sci. 33 (1998) 2771.
[13] F.H. Samuel, J. Mater. Sci. 33 (1998) 2283.
[14] P. Shewmon, P. Anderson, Acta Mater. 46 (1998) 4861.
[15] V. Kerlins, A. Phillips, in: Metals Handbook, 9th Ed., vol. 12, Fractography, American Society for Metals, Metals Park, OH, 1987, p. 12.
[16] B.A. Lerch, R.D. Noebe, K.B.S. Rao, J. Mater. Eng. Performance 7 (1998) 205.
[17] S.K. Sen, A. Ray, R. Avtar, S.K. Dhua, M.S. Prasad, P. Jha, P.P. Sengupta, S. Jha, J. Mater. Eng. Performance 7 (1998) 504.
[18] S.P. Lynch, Mater. Forum 11 (1988) 268.
[19] L. Liu, F.H. Samuel, J. Mater. Sci. 33 (1998) 2269.
[20] G. Han, J. He, S. Fukuyama, K. Yokogawa, Acta Mater. 46 (1998) 304.
[21] G. Arslar, M. Doruk, J. Mater. Sci. 33 (1998) 2653.
[22] S. Mrowec, M. Danielewski, A. Wojtowicz, J. Mater. Sci. 33 (1998) 2617.
[23] S.W. Paulik, S. Baskaran, T.R. Armstrong, J. Mater. Sci. 33 (1998) 2397.
[24] W. Rostoker, The Metallurgy of Vanadium, Wiley, New York, 1958, p. 139.
[25] W. Rostoker, A.S. Yamamoto, R.E. Riley, Trans. Am. Soc. Metals 48 (1956) 560.
[26] W. Rostoker, D.J. McPherson, M. Hansen, Wright air development center technical report 52-145, Part 2, 1954.
[27] W. Rostoker, M. Hansen, Wright Air Development Center technical report 52-145, Part 1, 1954.
[28] S.N. Votinov, M.I. Solonin, Y.I. Kazennov, V.P. Kondratjev, A.D. Nikulin, V.N. Tebus, E.O. Adamov, S.E. Bougaenko, Y.S. Strebkov, A.V. Sidorenkov, V.B. Ivanov, V.A. Kazakov, V.A. Evtikhin, I.E. Lyublinski, V.M. Trojanov, A.E. Rusanov, V.M. Chernov, G.A. Birgevoj, J. Nucl. Mater. 233–237 (1996) 370.
[29] D.L. Smith, H.M. Chung, B.A. Loomis, H.C. Tsai, J. Nucl. Mater. 237A (1996) 356.
[30] V.A. Evtikhin, I.E. Lyublinski, J. Adv. Mater. 1 (1994) 60.
[31] A.I. Dedyurin, L.I. Gomozov, S.N. Votinov, J. Phys. Chem. 5 (1983) 22.
[32] D.L. Smith, B.A. Loomis, D.R. Diercks, J. Nucl. Mater. 135 (1985) 125.
[33] H. Bohm, Nucl. Metall. 18 (1973) 163.
[34] B.A. Loomis, D.L. Smith, J. Nucl. Mater. 191 (1992) 84.
[35] K.C. Liu, J. Nucl. Mater. 103&104 (1981) 913.
[36] D.L. Harrod, R.E. Gold, Int. Met. Rev. 25 (1980) 163.
[37] H. Aglan, Int. J. Damage Mech. 2 (1993) 53.
[38] T.L. Anderson, Fracture Mechanics, CRC, Boca Raton, 1991, p. 305.
[39] J.E. King, Mater. Sci. Tech. 3 (1987) 750.
[40] M.S. Mirza, D.C. Barton, P. Church, J.L. Sturges, J. Phys. (Paris) IV 4 (1997) 891.
[41] T.D. Swankie, J.C.W. Davenport, D.J. Smith, Adv. Fract. Res. 1–6 (1997) 207.
[42] H. Aglan, Y. Gan, B.A. Chin, M.L. Grossbeck, J. Nucl. Mater. 273 (1999) 192.
[43] D. Broek, Elementary, Engineering Fracture Mechanics, Nijhoff (Martinus), Dordrecht, 1987, p. 269.
[44] F. Ellyin, Fracture Damage, Crack Growth and Life Prediction, Chapman and Hall, London, 1997, p. 18.
[45] Q.G. Wang, C.H. Caceres, J.R. Griffiths, Adv. Fract. Res. 1–6 (1997) 2511.
[46] W.F. Flanagan, B.D. Lichter, Int. J. Fract. 79 (1996) 121.
[47] E.I. Meletis, K. Lian, Int. J. Fract. 79 (1996) 165.

[48] R.L. Carlson, G.A. Kardomateas, An Introduction to Fatigue in Metals and Composites, Chapman and Hall, London, 1996, p. 137.
[49] T. Tanka, M. Jono, K. Komai, Current Research on Fatigue Cracks, Elsevier Applied Science, London, 1987, p. 27.
[50] H. Aglan, A. Othman, L. Figueroa, J. Mater. Sci. 29 (1994) 4786.
[51] H. Aglan, Z. Abdo, J. Adhes. Sci. Technol. 10 (1996) 183.